SUPPORTING INFORMATION

A new chemo-enzymatic approach to synthesize rare sugars using an engineered glycoside-3-oxidase

André Taborda[1], Márcia Rénio[1], M. Rita Ventura[1*] and Lígia O. Martins[1*]

[1]*Instituto de Tecnologia Química e Biológica António Xavier, Universidade Nova de Lisboa, Av da República, 2780-157 Oeiras, Portugal*

*Corresponding authors

Table of contents

Supplementary Figures

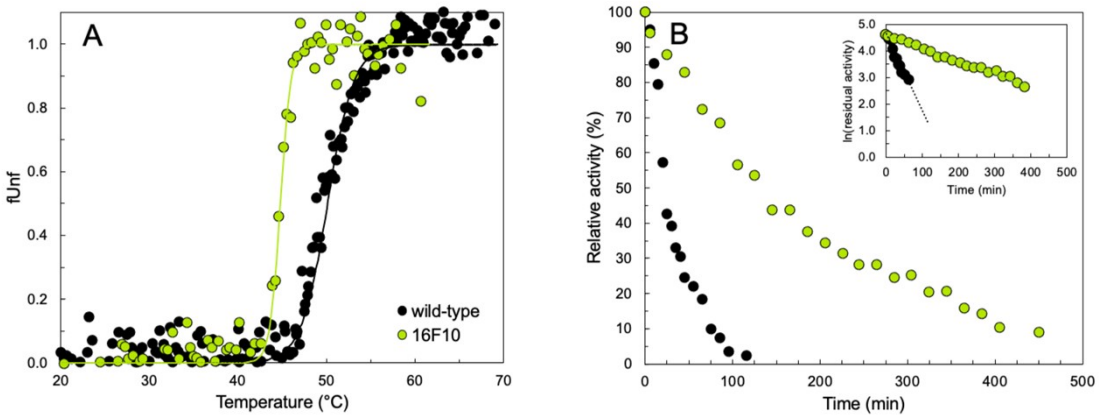

Fig. S1. Stability of the variant 16F10. (A) Comparison of thermostability between wild-type (black) and 16F10 variant (light green), assessed by steady-state fluorescence (Excitation at 296 nm and emission at 340 nm). The estimated apparent melting temperatures (T_m^{App}) were 49 ± 2 ºC for the wild-type and 44 ± 2 ºC for 16F10. **(B)** Thermal inactivation profile of wild-type (in black) and 16F10 (in light green) at 40 ºC. The residual activity was measured in a reaction mixture containing 0.5 M D-Glc, 0.1 mM AAP, 1 mM DCHBS, 8 U/ml HRP in 100 mM sodium phosphate buffer (pH 7.5). The inset shows the logarithm of residual activity versus incubation time. The obtained half-life at 40 ºC ($t_{1/2}^{40\ ºC}$) was 27 ± 2 min and 187 ± 30 min for the wild-type and 16F10, respectively.

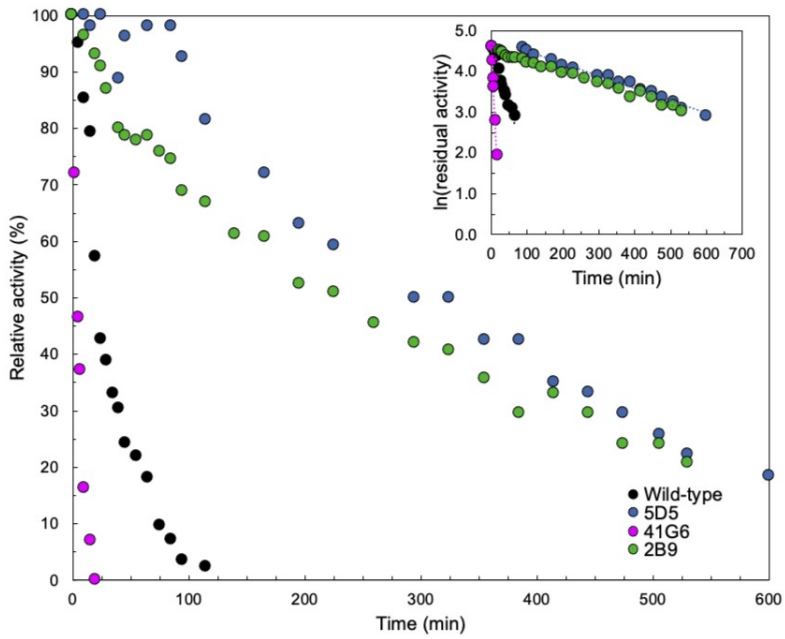

Fig. S2. Thermal inactivation at 40 ºC of some evolutionary intermediates (5D5, 41G6 and 2B9). The residual activity was measured in a reaction mixture containing 0.5 M D-Glc, 0.1 mM AAP, 1 mM DCHBS, 8 U/ml HRP in 100 mM sodium phosphate buffer (pH 7.5). The inset shows the logarithm of residual activity versus incubation time. The estimated half-life at 40 ºC ($t_{1/2}^{40\,ºC}$) was 27 ± 2 min for the wild-type (in black), 374 ± 82 min for 5D5 variant (in dark blue), 5 ± 1 min for 41G6 (in purple) and 291 ± 30 min for 2B9 (in green).

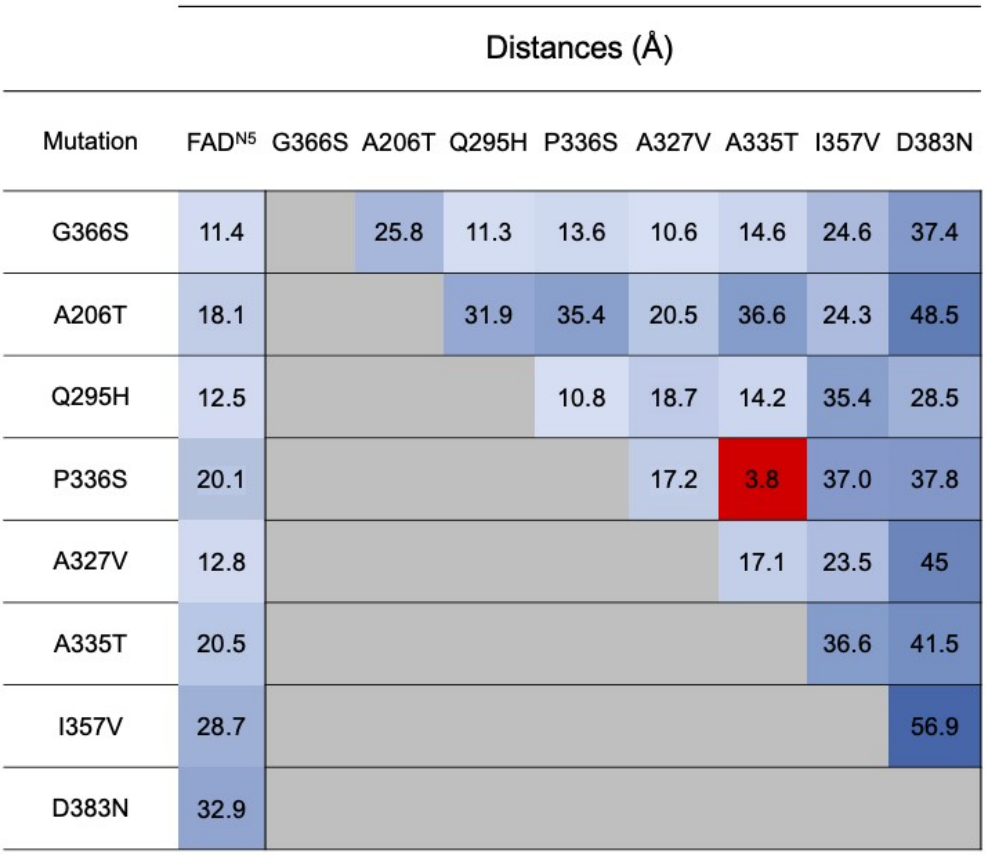

Fig. S3. Distances matrix among the mutations introduced in the hit variant 16F10 and between them and FAD. The distances are colored by a color gradient of red (lower distances) and blue (greater distances).

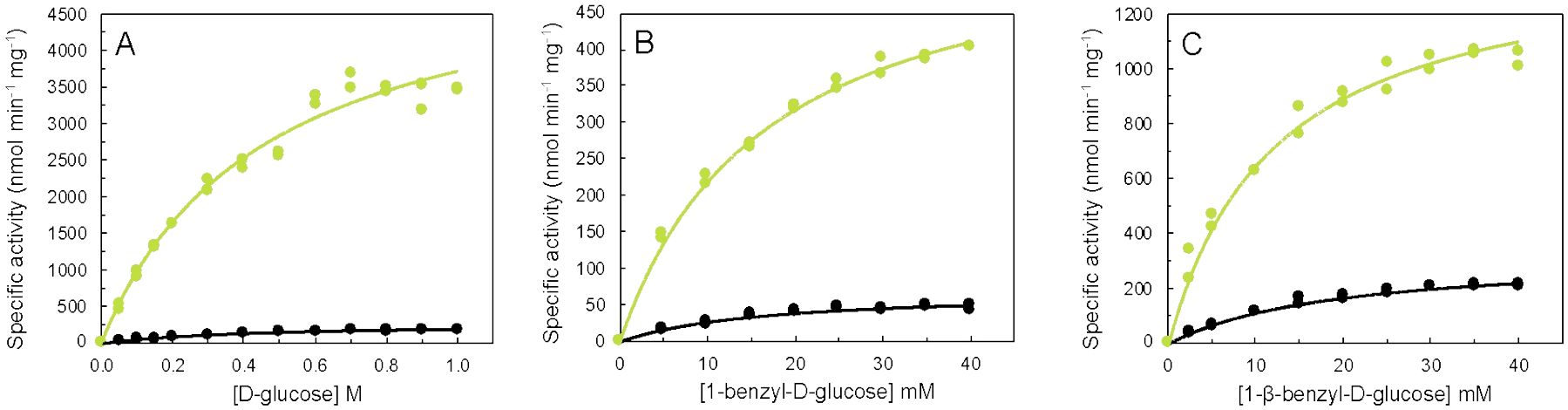

Fig. S4. Example of apparent steady-state kinetics of wild-type and 16F10 variant. Kinetics were obtained for **(A)** D-Glc, **(B)** 1-O-Benzyl-α/β-D-glucopyranoside and **(C)** 1-O-benzyl-β-glucopyranoside. The data in black correspond to the wild-type and in light green to 16F10 variant. All measurements were performed at 37 ºC in 100 mM sodium phosphate buffer at optimal pH using the HRP-AAP/DCHBS coupled assay**.** The dots represent the experimental enzymatic activities measured, and the lines are the fit of the experimental data to the Michaelis-Menten equation using OriginLab software.

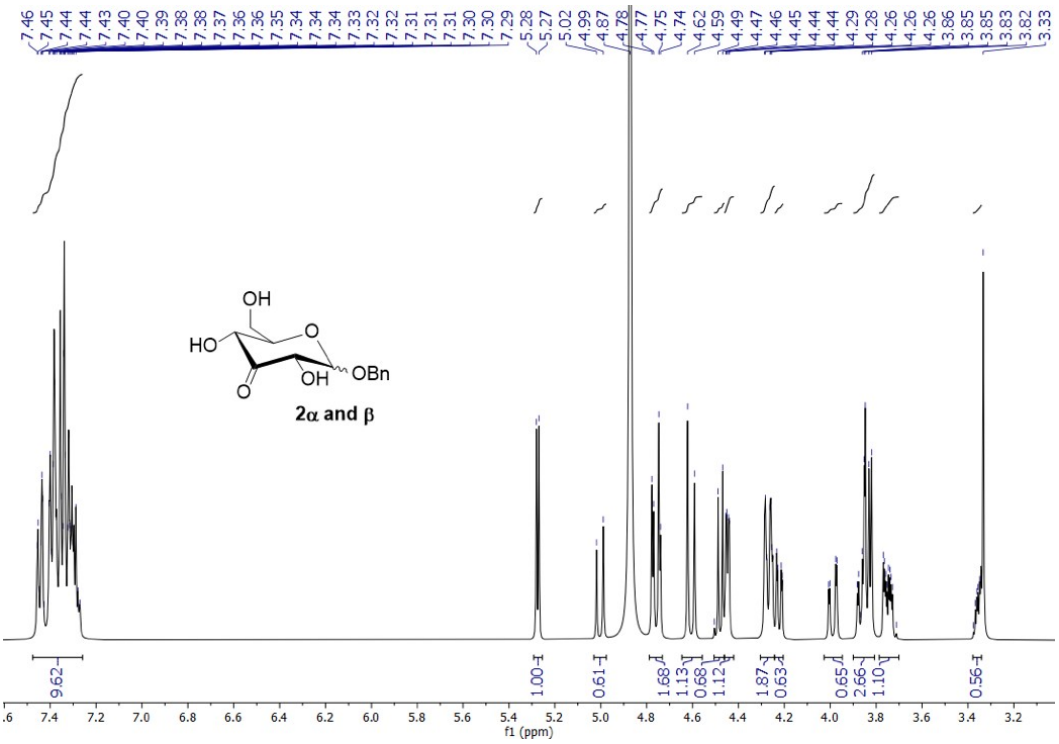

Fig. S5. ^{1}H NMR spectrum of 1-O-Benzyl-3-keto-α/β-D-glucopyranoside 2α and 2β.

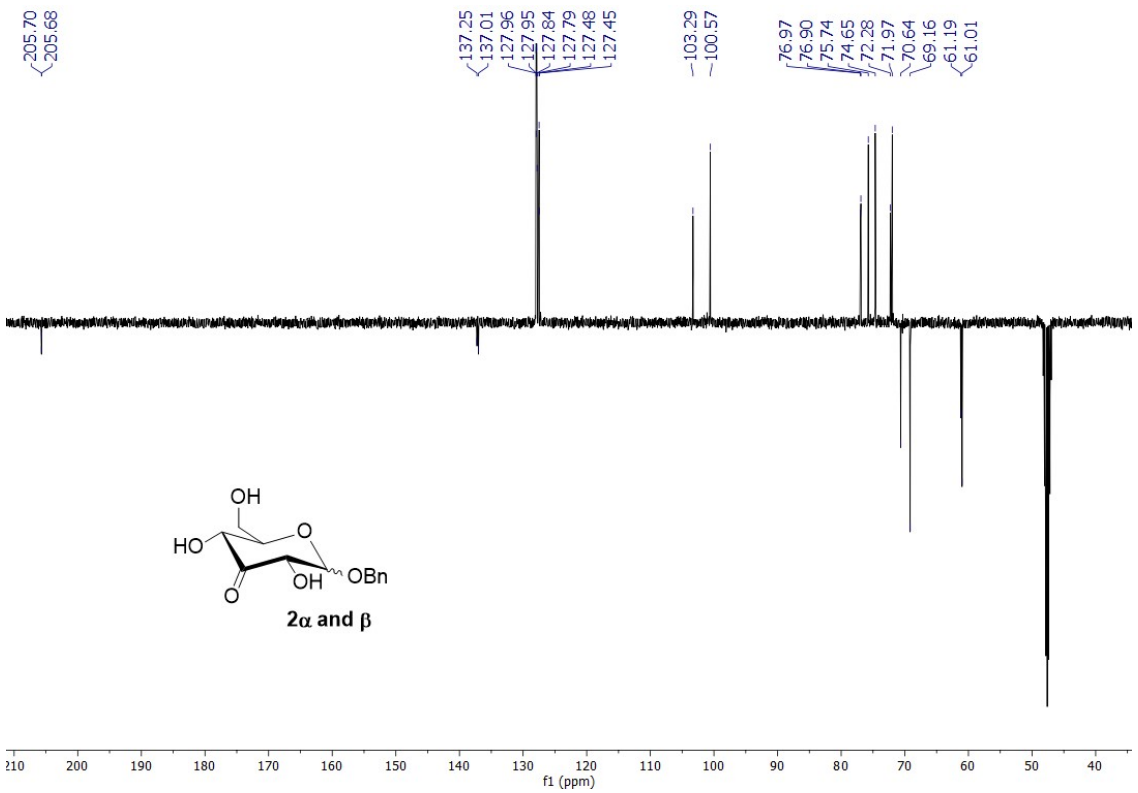

Fig. S6.[13]C NMR spectrum of 1-O-Benzyl-3-keto-α/β-D-glucopyranoside 2α and 2β.

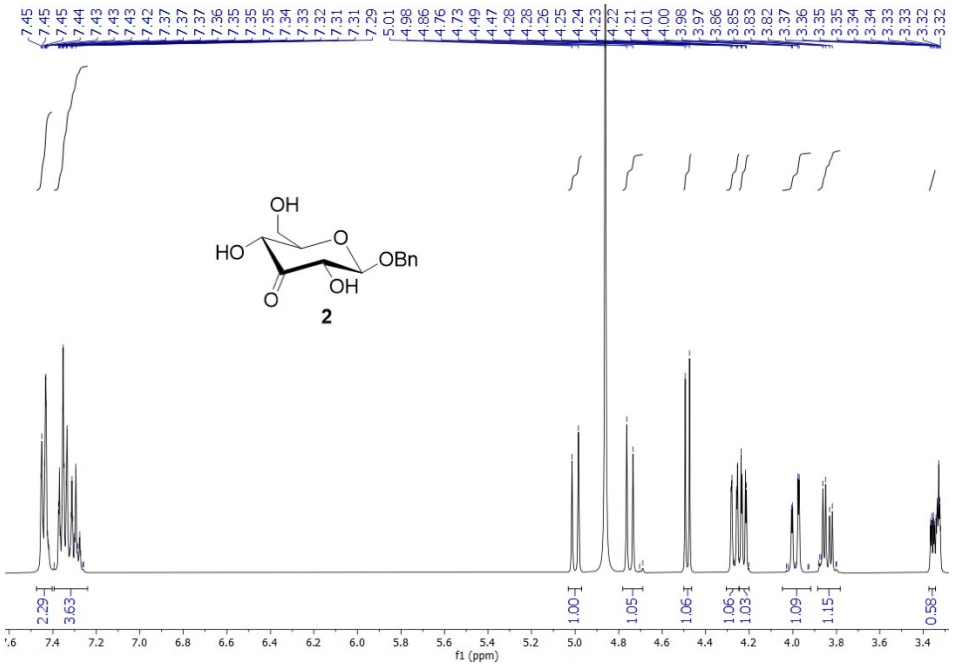

Fig. S7.[1]H NMR spectrum of 1-O-Benzyl-3-keto-β-D-glucopyranoside 2β anomer**.**

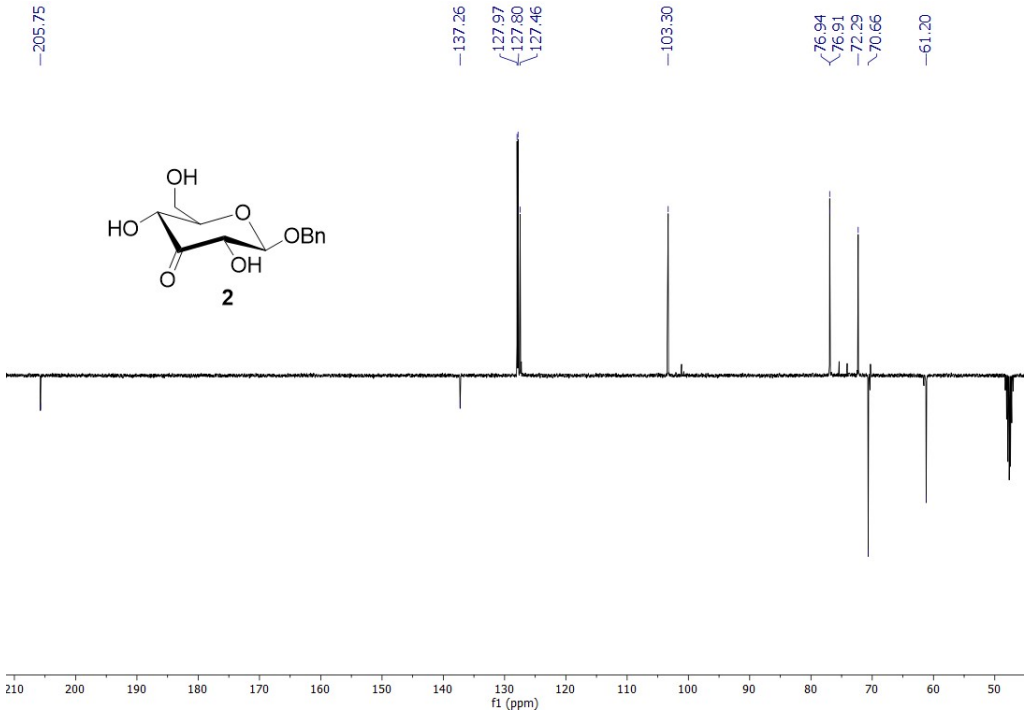

Fig. S8. ^{13}C NMR spectrum of 1-O-Benzyl-3-keto-β-D-glucopyranoside 2β.

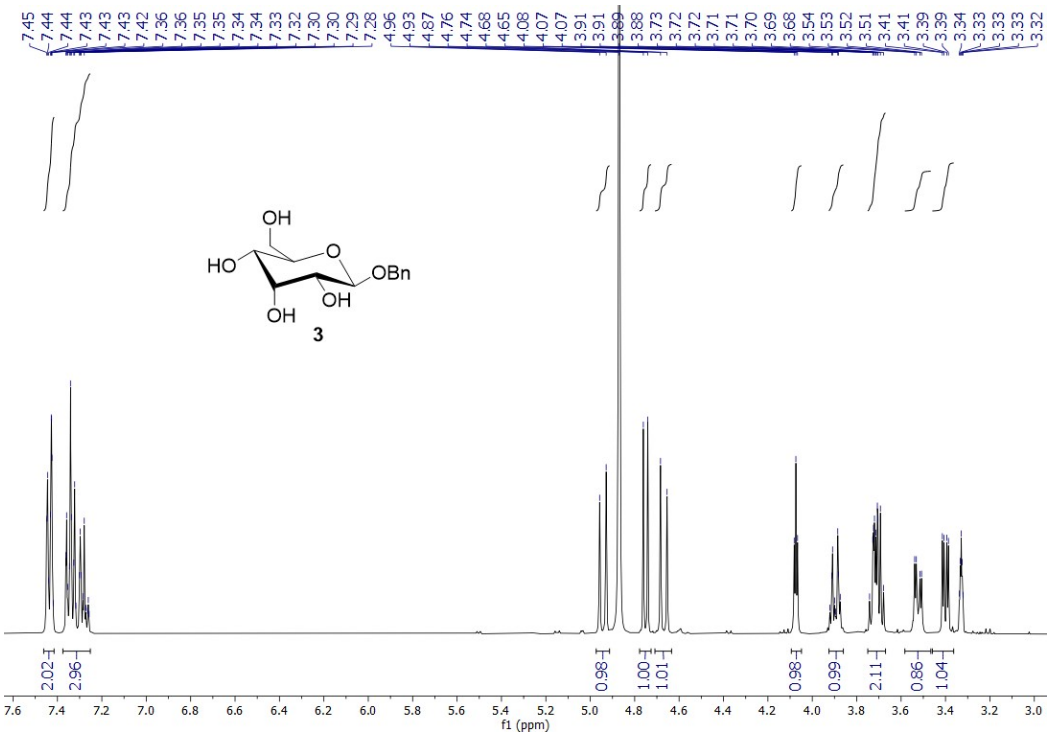

Fig. S9. ^{1}H NMR spectrum of 1-O-Benzyl-β-D-allopyranoside 3.

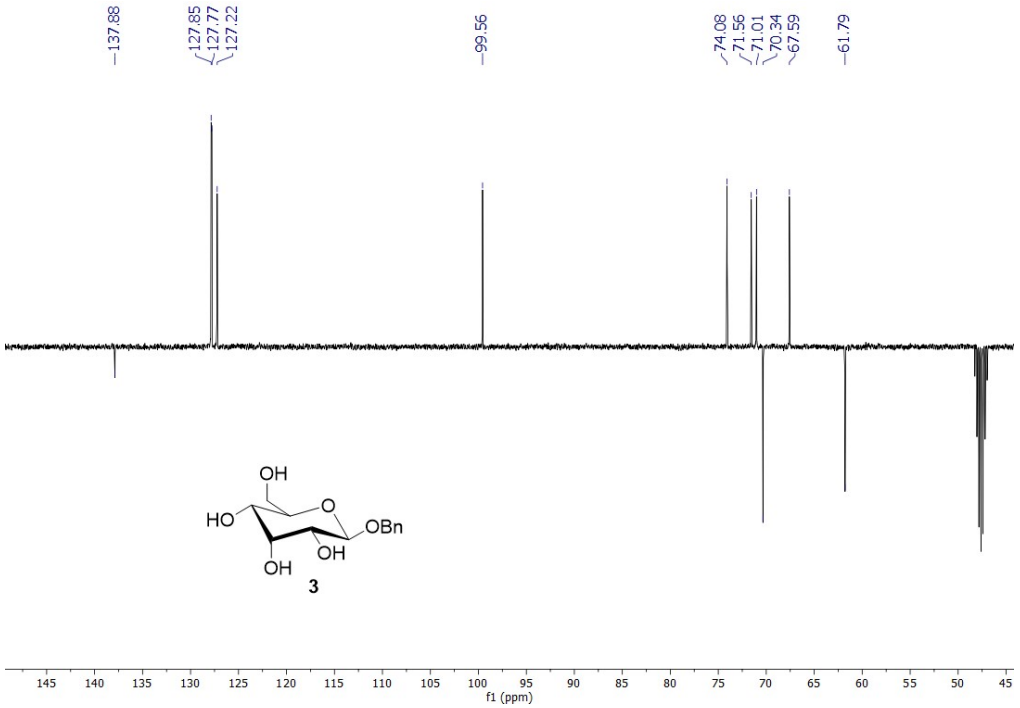

Fig. S10. ^{13}C NMR spectrum of 1-O-Benzyl-β-D-allopyranoside 3.

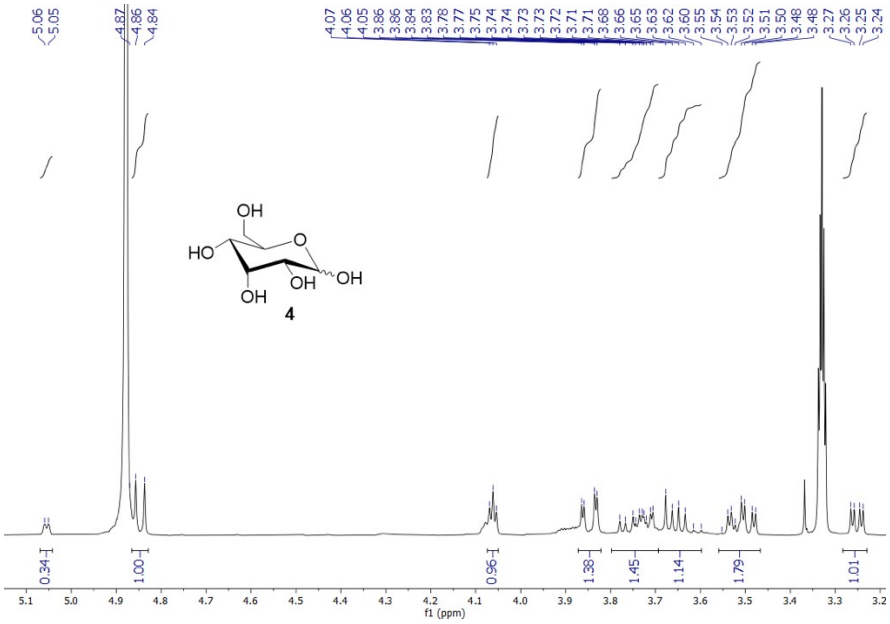

Fig. S11. ^{1}H NMR spectrum of D-allose 4.

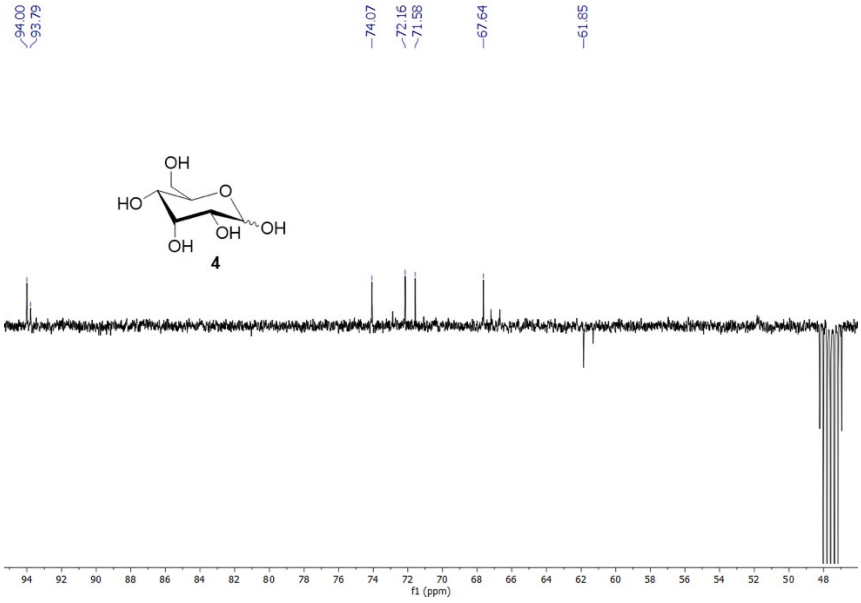

Fig. S12. ^{13}C NMR spectrum of D-allose 4.

Supplementary Tables

Table S1. Bacterial strains, plasmids, and primers were used in this study. F indicates forward primers, and R reverse primers.

Strains, Plasmids, or Primers	Genotype, property, or sequence	Reference or source
Strains		
E. coli DH5α	F⁻ φ80*lac*ZΔM15 Δ(*lac*ZYA a*rg*F)U169 *rec*A1 *end*A1 *hsd*R17(r_K^-, m_K^+) *pho*A *sup*E44 λ⁻ *thi*-1 *gyr*A96 *rel*A1	Novagen
E. cloni 10G elite	F⁻ mcrA Δ(mrr-hsdRMS-mcrBC) endA1 recA1 φ80dlacZΔM15 ΔlacX74 araD139 Δ(ara,leu)7697 galU galK rpsL (StrR) nupG λ− tonA	Lucigen corporation – Biosearch Technologies
E. coli KRX	[F′, *tra*D36, D*omp*P, *roa*⁺B⁺, *lac*I^q, D(*lac*Z)M15] D*omp*T, *end*A1, *rec*A1, *gyr*A96 (Nal^r), *thi*-1, *hsd*R17 (r_K^-, m_K^+), e14⁻ (McrA⁻), *rel*A1, *sup*E44, D(*lac-pro*AB), D(*rha*BAD)::T7 RNA polymerase	Promega
E. coli Rosetta(DE3) pLysS	F⁻ ompT hsdSB(rB⁻ mB⁻) gal dcm (DE3) pLysSRARE (CamR)	Novagen
Plasmids		
pET15b	Cloning vector with a T7 promoter with a N-terminal T7tag and C-terminal 6xHis tag; amp^r	Novagen
pSM1	pET15b with *psg3ox* gene cloned into *Nde*I and *XhoI* sites	[1]
pAT-3	pET15b with *psg3ox* gene cloned into *Nde*I and *XhoI* sites carrying the mutation A75T introduced in the by site-directed mutagenesis	This work
pAT-4	pET15b with *psg3ox* gene cloned into *Nde*I and *XhoI* sites carrying the mutation A206T introduced in the by site-directed mutagenesis	This work
pAT-5	pET15b with *psg3ox* gene cloned into *Nde*I and *XhoI* sites carrying the mutation Q295H introduced in the by site-directed mutagenesis	This work
pAT-6	pAT-1A1 with *psg3ox* gene cloned into *Nde*I and *XhoI* sites carrying the mutation G366S and Q295H introduced in the by site-directed mutagenesis	This work
pAT-9	pET15b with *psg3ox* gene cloned into *Nde*I and *XhoI* sites carrying the mutation S336P introduced in the by site-directed mutagenesis	This work
pAT-10	pAT-2G4 with *psg3ox* gene cloned into *Nde*I and *XhoI* sites carrying the mutation P336S introduced in the by site-directed mutagenesis	This work
pAT-11	pAT-7E9 with *psg3ox* gene cloned into *Nde*I and *XhoI* sites carrying the mutation P336S introduced in the by site-directed mutagenesis	This work

pAT-12	pAT-2B9 with *psg3ox* gene cloned into *Nde*I and *XhoI* sites carrying the mutation P336S introduced in the by site-directed mutagenesis	This work
pAT-1A1	pET15b with *psg3ox* gene cloned into *Nde*I and *XhoI* sites carrying the mutation G366S introduced in the first round of directed evolution	This work
pAT-5D5	pET15b with *psg3ox* gene cloned into *Nde*I and *XhoI* sites carrying the mutation G366S, A75T, A206T, Q295H introduced in the second round of directed evolution	This work
pAT-41G6	pET15b with *psg3ox* gene cloned into *Nde*I and *XhoI* sites carrying the mutation G366S, A75T, A206T, Q295H, P336S introduced in the third round of directed evolution	This work
pAT-7E9	pET15b with *psg3ox* gene cloned into *Nde*I and *XhoI* sites carrying the mutation G366S, A75T, A206T, Q295H, P336S, D222G, A327V introduced in the fourth round of directed evolution	This work
pAT-2G4	pET15b with *psg3ox* gene cloned into *Nde*I and *XhoI* sites carrying the mutation G366S, A75T, A206T, Q295H, P336S, A327V, V416I, K420R introduced in the fourth round of directed evolution	This work
pAT-2B9	pET15b with *psg3ox* gene cloned into *Nde*I and *XhoI* sites carrying the mutation G366S, A75T, A206T, Q295H, P336S, D222G, A327V, V416I, K420R, A335T introduced in the fifth round of directed evolution	This work
pAT-6E3	pET15b with *psg3ox* gene cloned into *Nde*I and *XhoI* sites carrying the mutation G366S, A206T, Q295H, P336S, A327V, A335T introduced in the sixth round of directed evolution	This work
pAT-16F10	pET15b with *psg3ox* gene cloned into *Nde*I and *XhoI* sites carrying the mutation G366S, A206T, Q295H, P336S, A327V, A335T, D383N, I357V introduced in the seventh round of directed evolution	This work
Primers		
*Ps*G3Ox_A75T_FW	5’-GGGTCCCGGTACCGGTGCTGCAACAGTG-3'	This work
*Ps*G3Ox_A75T_RV	5’-CACTGTTGCAGCACCGGTACCGGGACCC-3'	This work
*Ps*G3Ox_A206T_FW	5’-GCAGGATGGCACCCTCGTATGGTCCGGCTC-3'	This work
*Ps*G3Ox_A206T_RV	5’-GAGGCCGGACCATACGAGGGTGCCATCCTGC-3'	This work
*Ps*G3Ox_Q295H_FW	5’-CTGAACGACCATGCGCAGGTGGTGTTCGCG-3'	This work
*Ps*G3Ox_Q295H_RV	5’-CGCGAACACCACCTGCGCATGGTCGTTCAG -3'	This work
*Ps*G3Ox_P336S_FW	5’-CGGACGAGGCGTCCTTCCACGGCCAGATC-3'	This work
*Ps*G3Ox_P336S_RV	5’-GATCTGGCCGTGGAAGGACGCCTCGTCCG-3'	This work
*Ps*G3Ox_S336P_FW	5’-CGGACGAGGCGCCCTTCCACGGCCAGATC-3'	This work
*Ps*G3Ox_S336P_RV	5’-GATCTGGCCGTGGAAGGGCGCCTCGTCCG-3'	This work
pET21_FW	5’-CTTCCCCATCGGTGATGTCGGCGATATAG-3'	This work
pET21_RV	5’-CCAAGGGGTTATGCTAGTTATTGCTCAG-3’	This work
*Ps*G3Ox_GA_FW	5’-GCAGCCGGATCCTCGAGCATTATTTAGACAGTCTATTGTCTGATTCGG-3'	This work

*Ps*G3Ox_GA_RV	5’-TGGTGCCGCGCGGCAGCCATATGAGCGGTCACCGGTATC-3'	This work
pET15b_GA_FW	5’-ATGGCTGCCGCGCGGCAC-3'	This work
pET15b_GA_RV	5’-ATGCTCGAGGATCCGGCTG-3'	This work

Table S2. Programs carried out in thermocycler for the PCRs performed in this study.

	Program 1 (error-prone PCR and last PCR of DNA shuffling)	**Program 2** (vector for epPCR libraries)	**Program 3** (First PCR for DNA shuffling – gene amplification)	**Program 4** (Primerless PCR for DNA shuffling – reassembly)	**Program 5** (Site-directed mutagenesis)
Initial denaturation	95 ºC – 2 min	98 ºC – 30s	95 ºC – 5 min	96 ºC – 3 min	95 ºC – 4 min
Cycles (Denaturation, Annealing, Extension)	30 cycles 95 ºC – 1 min 69 ºC – 1 min 72 ºC – 2 min	30 cycles 98 ºC – 10s 71 ºC – 30s 72 ºC – 3min	20 cycles 95 ºC – 1 min 55 ºC – 1min 72 ºC – 2 min	45 cycles 94 ºC – 1min 59 ºC - 1.5 min 56 ºC – 1.5 min 53 ºC – 1.5 min 50 ºC – 1.5 min 47 ºC – 1.5 min 44 ºC – 1.5 min 41 ºC – 1.5 min 72 ºC – 1min + 5s/cycle	20 cycles 95 ºC – 1 min 68 ºC – 1.5 min 72 ºC – 8 min
Final extension	72 ºC – 10 min	72 ºC – 2 min	72 ºC – 10 min	72 ºC – 10 min	72 ºC – 10 min

Table S3. Summary of the variants obtained by directed evolution. The concentration of the mutagenic agent ($MnCl_2$) in the epPCR is mentioned for each round of evolution performed. The concentration of substrate (D-Glc) used in the screenings, the number of variants screened in both applied screening approaches ('Activity-on-plate/96-well plate screenings) and the relative activity and stability values to the respective parent are presented. N.D. means not determined.

Generation	**[$MnCl_2$]** mM	**[D-Glc]** mM	**# Screened variants**	**Variant**	**Mutations**	**Relative Activity**	**Relative Stability**
1st	0.05	500	7500/100	**1A1**	G366S	3.7 ± 0.9	N.D.
2nd	0.05	100	4000/900	**5D5**	G366S, A75T, A206T, Q295H	5.0 ± 0.9	N.D.
3rd	0.05/ 0.1	100	10000/2000	**41G6**	G366S, A75T, A206T, Q295H, P336S	2.3 ± 0.8	N.D.
4th	0.1	50	5900/600	**2G4**	G366S, A75T, A206T, Q295H, P336S, A327V, V416I, K420R	2.5 ± 0.5	N.D.
				7E9	G366S, A75T, A206T, Q295H, P336S, A327V, D222G	2.4 ± 0.4	N.D.
5th (epPCR + shuffling)	0.1	50	5100/500	**2B9**	G366S, A75T, A206T, Q295H, P336S, A327V, K420R, V416I, D222G, A335T	1.0 ± 0.2	3.7 ± 0.6
6th (Shuffling wt/2B9)	-	50	2500/600	**6E3**	G366S, A206T, Q295H, P336S, A327V, A335T	1.3 ± 0.2	1.2 ± 0.1
				1F3	G366S, A75T, A206T, Q295H, P336S, A327V, A335T	1.4 ± 0.1	0.9 ± 0.1
				1D3	G366S, A206T, Q295H, P336S, A327V, D222G A335T	1.3 ± 0.1	1.3 ± 0.2
				5F3	G366S, A206T, Q295H, P336S, A327V, A335T, V416I, K420R	1.0 ± 0.2	1.1 ± 0.1
				11G7	G366S, A206T, Q295H, P336S, A327V, D222G, A335T, V416I	0.8 ± 0.1	1.3 ± 0.2
7th	0.1	50	11200/1750	**16F10**	G366S, A206T, Q295H, P336S, A327V, A335T, I357V, D383N	1.6 ± 0.3	1.3 ± 0.1

Table S4. Summary of production yields for all directed evolution intermediates. The Bradford method was used to determine the total concentration of enzyme. Functional enzyme concentration was quantified by absorbance at 450 nm.

Variant	**Production yield** (mg/L culture)	**Ratio functional/ total enzyme**
Wild-type	30	20 %
1A1	62	25 %
5D5	97	24 %
41G6	35	40 %
2G4	20	50 %
7E9	30	30 %
2B9	35	55 %
6E3	33	35 %
16F10	37	37 %

Table S5. Apparent steady-state catalytic parameters for D-Glc in pyranose oxidases described in literature. nd - not detected

Origin	Microorganism	Enzyme	k_{cat} (s^{-1})	K_m (M)	k_{cat}/K_m ($M^{-1}s^{-1}$)	Ref.
Bacterial	*Pseudarthrobacter siccitolerans*	*Ps*G3Ox	0.2	0.4	0.5	[2]
	Kitasatospora aureofaciens	*Ka*P2Ox	15.4	1.5×10^{-3}	1.0×10^{4}	[3]
	Microbacterium sp. 5-2b	CarA	nd	-	-	[4]
	Arthrobacter globiformis	*Ag*CarA	nd	-	-	[4]
	Microbacterium trichotheecenolyticum	*Mt*CarA	nd	-	-	[4]
	Streptomyces canus	*Sc*P2Ox	> 0.38	> 2.0	> 0.19	[5]
Fungal	*Phlebiopsis gigantea*	*Phg*P2Ox	40.5	1.2×10^{-3}	3.4×10^{4}	[6]
	Trametes multicolor	*Tm*P2Ox	54.0	0.7×10^{-3}	7.3×10^{4}	[7]
	Tricholoma matsutake	*Tma*P2Ox	111.0	1.3×10^{-3}	8.7×10^{4}	[8]
	Peniophora gigantea	*Peg*P2Ox	56	1.1×10^{-3}	5.0×10^{4}	[9]
	Peniophora sp.	*Ps*P2Ox	9.4	5.0×10^{-3}	1.8×10^{3}	[10]
	Phanerochaete chrysosporium	*Pc*P2Ox	83.1	0.8×10^{-3}	9.9×10^{4}	[11]
	Lyophyllum shimeji	*Ls*P2Ox	6.9	0.3×10^{-3}	2.2×10^{4}	[12]
	Aspergillus nidulans	*An*P2Ox	35.4	1.8×10^{-3}	2.0×10^{4}	[13]
	Aspergillus oryzae	*Ao*P2Ox	1.5	2.9×10^{-3}	0.5×10^{3}	[13]
	Irpex lacteus	*Il*P2Ox	33.8	0.7×10^{-3}	4.6×10^{4}	[14]

Table S6. Optimal pH and apparent steady-state catalytic parameters for D-Glc of variants where mutation P336S was inserted (wild-type) or removed (2G4, 7E9 and 2B9) considered in this study. Activity was measured using the HRP-AAP/DCHBS coupled assay. All reactions were performed in 100 mM sodium phosphate buffer at the optimal pH and 37 ºC. The kinetic parameters were determined by fitting the data directly on the Michaelis-Menten equation using OriginLab.

Enzyme	Mutations	Optimal pH	k_{cat} (s^{-1})	K_m (M)	k_{cat}/K_m ($M^{-1}s^{-1}$)
wild-type	-	7.0 – 7.5	0.2 ± 0.05	0.37 ± 0.13	0.5 ± 0.1
P336S	+ P336S	7.5 - 8.5	0.2 ± 0.03	0.54 ± 0.11	0.3 ± 0.02
2G4	K420R; V416I; A327V; P336S; A75T; A206T; Q295H; G366S	8.0	1.9 ± 0.2	0.26 ± 0.05	6.7 ± 0.8
2G4 (-P336S)	K420R; V416I; A327V; A75T; A206T; Q295H; G366S	8.0 - 8.5	0.8 ± 0.1	0.28 ± 0.03	2.8 ± 0.5
7E9	A327V; D222G; P336S; A75T; A206T; Q295H; G366S	8.0	2.3 ± 0.3	0.27 ± 0.05	8.6 ± 0.4
7E9 (-P336S)	A327V; D222G; A75T; A206T; Q295H; G366S	8.0 - 8.5	1.0 ± 0.1	0.28 ± 0.03	3.6 ± 0.3
2B9	A335T; K420R; V416I; A327V; D222G; P336S; A75T; A206T; Q295H; G366S	8.0	2.6 ± 0.3	0.23 ± 0.06	10.6 ± 0.9
2B9 (-P336S)	A335T; K420R; V416I; A327V; D222G; A75T; A206T; Q295H; G366S	8.0 - 8.5	0.7 ± 0.1	0.24 ± 0.02	3.0 ± 0.2

Table S7. Summary of stability properties of the evolutionary intermediates. Apparent melting temperatures (T_m^{App}) were measured by steady-state fluorescence following the intrinsic fluorescence of the enzyme, aggregation temperature (T_{agg}) was monitored by static light scattering and half-life time at 40ºC ($t_{1/2}^{40ºC}$) was measured by following the loss activity over time. The activity at each time point was measured using the HRP-AAP/DCHBS system.

Variant	T_m^{App} (ºC)	T_{agg} (ºC)	$t_{1/2}^{40ºC}$ (min)
WT+P336S	47 ± 2	45	Not detected
2G4-P336S	55 ± 2	53	990 ± 110
7E9-P336S	56 ± 2	54	2310 ± 260
2B9-P336S	56 ± 3	55	990 ± 213

Table S8. Optimal pH and apparent steady-state catalytic parameters for D-Glc of variants constructed using site-directed mutagenesis to assess the role of mutations G366S, A75T, A206T and Q295H. Activity was measured using the HRP-AAP/DCHBS coupled assay. All reactions were performed in 100 mM sodium phosphate buffer at the optimal pH and 37 ºC. The kinetic parameters were determined by fitting the data directly on the Michaelis-Menten equation using OriginLab.

Enzyme	Mutation	Optimal pH	k_{cat} (s^{-1})	K_m (M)	k_{cat}/K_m ($M^{-1}s^{-1}$)
wild-type	-	7.0 – 7.5	0.2 ± 0.05	0.37 ± 0.13	0.5 ± 0.1
1A1	G366S	7.5	0.4 ± 0.1	0.54 ± 0.11	0.7 ± 0.1
wild-type	+ A75T	7.5	0.2 ± 0.03	0.59 ± 0.14	0.4 ± 0.1
wild-type	+A206T	7.5	0.3 ± 0.03	0.56 ± 0.05	0.5 ± 0.1
wild-type	+Q295H	8.5	0.5 ± 0.02	0.28 ± 0.02	1.8 ± 0.1
wild-type	+Q295H/G366S	8.5	0.9 ± 0.03	0.28 ± 0.02	3.2 ± 0.3
5D5	A75T; A206T; Q295H; G366S	8.5	1.0 ± 0.2	0.33 ± 0.05	3.2 ± 0.4

Table S9. Summary of the described methods for synthetizing 3-keto-sugars and D-allose. In the case of methods that use enzymes the abbreviations used are: G3Ox- Glycoside-3-oxidase; RPI- Ribose-5-phosphate isomerase; DAE- D-allulose-3-epimerase; GI- Glucose isomerase.

Method	Substrate	Temp. (°C)	Number of steps (chemical or enzymatic)	Yield (%)	Enzymes	Chemicals used (other than solvents)	Product	Byproducts	Additional information	Ref.
Chemo-enzymatic (D-allose)	1-O-benzyl-β-D-glucopyranoside	25 / 0	3 (oxidation; reduction; deprotection)	81	G3Ox	LS-selectride, Pd/C	D-allose	n.d.	No final purification is required.	This work
Chemosynthesis (3-keto-sugars)	semi-protected saccharides	r.t.	1 (oxidation)	45-96	none	[(2,9-dimethyl-1,10-phenanthroline)-Pd(m-OAc)]$_2$(OTf)$_2$, benzoquinone	3-keto-derivatives	n.d.	-	15
	semi-protected monosaccharides	50	1 (oxidation)	>92	none	[(neocuproine)Pd-(OAc)]$_2$(OTf)$_2$, benzoquinone	3-keto-derivatives	C4 oxidized product	A mixture of C3/C4 oxidation products is obtained for some substrates.	16
	semi-protected monosaccharides	25	1 (oxidation)	21-70	none	Quinuclidine, Me_4NBF_4, HFIP, MeCN	3-keto-derivatives	n.d.	For some substrates, 6-OH needs to be protected. Requires graphite electrodes.	17
Chemosynthesis (D-allose)	D-ribose	n.i.	2 (cyanohydrin reaction; reduction)	n.i.	none	Sodium amalgam, HCN, NaCN	D-allose	D-altronate	-	18
	3-keto-sucrose	30	2 (reduction; bacterial hydrolysis)	63	none	Raney nickel	D-allose	n.d.	A bacterial strain was used to hydrolyze the glycosidic bond of the formed intermediate allosylfructose	19
	1,2 5,6-dl-O-lsopropyhdene-a-D-glucofuranose	25	2 (reduction, hydrolysis)	70	none	KIO_4, K_2CO_3, RuO_2 $NaBH_4$	D-allose	n.i.	This method requires specific chromatographic steps.	20
	D-glucose	n.i.	1 (epimerization)	>7	none	Molybdenum	D-allose	n.i.	-	21
	D-glucose	120	1 (epimerization)	14	none	$(NH_4)_2MoO_4$ CH_3COOH	D-allose	D-altrose	The final mixture was incubated with *S. cerevisiae* to remove residual glucose and mannose—complex purification.	22
	D-glucose	r.t. / 0	2 (oxidation, reduction)	54	none	[(neocuproine)Pd-(OAc)]$_2$(OTf)$_2$, benzoquinone, $NaBH_4$	D-allose	D-glucose	The reduction step originates a mix of allose/glucose	23
	D-glucose	r.t.	1 (epimerization)	42	none	4-CzlPN, quinuclidine, Ad-SH, 4-ClOBzBu$_4$N	D-allose	n.d.	Require a blue LED lamp.	24
Biosynthesis (D-allose) – Izumoring	D-allulose [a]	65	1 (one step transformation)	32	RPI	-	D-allose (not isolated)	n.d.	Low yields obtained due to the enzyme's reversibility. The substrate is expensive.	25
	D-fructose [b]	60	2 (two-step transformation - 'one-pot')	13	DAE, RPI	-	D-allose (not isolated)	D-allulose	Low yields due to the enzyme's reversibility	26
	D-glucose [c]	30	1 (*in vivo* fermentation – *E. coli*)	n.i.	GI, DAE, RPI	-	D-allose (not isolated)	D-allulose, D-fructose	Low yields due to the enzyme's reversibility. The substrate can be utilized in *E. coli* metabolic pathways.	27

r.t. - room temperature; n.i. - not indicated; n.d. - not detected.

[a] - There are other isomerase enzymes capable of converting D-allulose to D-allose. Still, like in this case, they remain reversible, leading to low yields and requiring product purification afterward to remove byproducts and/or the remaining initial substrate (The conversion yields range from 25% to 37.5% [28]).

[b] – Other epimerases and isomerases have also been used to convert D-fructose to D-allose, employing both one-pot reactions and sequential two-step processes. However, due to the reversibility of the system, yields remain similar (ranging from 10% to 13% [28]), and product purification is still required to remove the starting substrate.

[c] – Although the authors do not provide the production's quantitative yield, they mention it was 'quite low.'

References

1. S. Mendes, C. Banha, J. Madeira, D. Santos, V. Miranda, M. Manzanera, M. R. Ventura, W. J. H. van Berkel and L. O. Martins, *J Mol Catal B Enzym*, 2016, **133**, S34-S43.
2. A. Taborda, T. Frazão, M. V. Rodrigues, X. Fernández-Luengo, F. Sancho, M. F. Lucas, C. Frazão, E. P. Melo, M. R. Ventura, L. Masgrau, P. T. Borges and L. O. Martins, *Nat Commun*, 2023, **14**, 7289.
3. P. L. Herzog, L. Sützl, B. Eisenhut, D. Maresch, D. Haltrich, C. Obinger and C. K. Peterbauer, *Appl Environ Microbiol*, 2019, **85**, 1-15.
4. T. Kumano, S. Hori, S. Watanabe, Y. Terashita, H. Y. Yu, Y. Hashimoto, T. Senda, M. Senda and M. Kobayashi, *Proc Nat Acad Sci*, 2021, **118**, e2106580118.
5. A. Kostelac, L. Sützl, J. Puc, V. Furlanetto, C. Divne and D. Haltrich, *Int J Mol Sci*, 2022, **23**, 13595.
6. A. Schafer, S. Bieg, A. Huwig, G. Kohring and F. Giffhorn, *Appl Environ Microbiol*, 1996, **62**, 2586-2592.
7. C. Leitner, J. Volc and D. Haltrich, *Appl Environ Microbiol*, 2001, **67**, 3636-3644.
8. Y. Takakura and S. Kuwata, *Biosci Biotechnol Biochem*, 2003, **67**, 2598-2607.
9. S. Bastian, M. J. Rekowski, K. Witte, D. M. Heckmann-Pohl and F. Giffhorn, *Appl Microbiol Biotechnol*, 2005, **67**, 654-663.
10. M. Bannwarth, D. Heckmann-Pohl, S. Bastian, F. Giffhorn and G. E. Schulz, *Biochem*, 2006, **45**, 6587-6596.
11. I. Pisanelli, M. Kujawa, O. Spadiut, R. Kittl, P. Halada, J. Volc, M. D. Mozuch, P. Kersten, D. Haltrich and C. Peterbauer, *J Biotechnol*, 2009, **142**, 97-106.
12. C. Salaheddin, Y. Takakura, M. Tsunashima, B. Stranzinger, O. Spadiut, M. Yamabhai, C. K. Peterbauer and D. Haltrich, *Microb Cell Fact*, 2010, **9**, 1-12.
13. I. Pisanelli, P. Wührer, Y. Reyes-Dominguez, O. Spadiut, D. Haltrich and C. Peterbauer, *Appl Microbiol Biotechnol*, 2012, **93**, 1157-1166.
14. M. Q. Ai, F. F. Wang, Y. Z. Zhang and F. Huang, *Process Biochem*, 2014, **49**, 2191-2198.
15. M. Jäger, M. Hartmann, J. G. de Vries and A. J. Minnaard, *Angew Chem Int Ed*, 2013, **52**, 7809-7812.
16. K. Chung and R. M. Waymouth, *ACS Catal*, 2016, **6**, 4653-4659.
17. M. Kidonakis, A. Villotet, M. D. Witte, S. B. Beil and A. J. Minnaard, *ACS Catal*, 2023, **13**, 2335-2340.
18. F. P. Phelps and F. Bates, *J. Am. Chem. Soc.*, 1934, **56**, 1250-1250.
19. M. J. Bernaerts, J. Furnelle and J. De Ley, *Biochim Biophys Acta*, 1963, **69**, 322-330.
20. D. C. Baker, D. Horton and C. G. Tindall, *Carbohydr Res*, 1972, **24**, 192-197.
21. *United States Pat.,* US5433793A, 1994.
22. V. Bílik and I. Knězek, *Chem Papers*, 1988, **42**, 401-405.
23. V. R. Jumde, N. N. H. M. Eisink, M. D. Witte and A. J. Minnaard, *J Org Chem*, 2016, **81**, 11439-11443.
24. Y. Wang, H. M. Carder and A. E. Wendlandt, *Nature*, 2020, **578**, 403-408.
25. S. J. Yeom, E. S. Seo, Y. S. Kim and D. K. Oh, *Appl Microbiol Biotechnol*, 2011, **89**, 1859-1866.
26. T. E. Lee, K. C. Shin and D. K. Oh, *J Microbiol Biotechnol*, 2018, **28 3**, 418-424.
27. L. Zheng, Q. Guo, Y. Zhang, C. Liu, L. Fan and H. Zheng, *Front. Bioeng. Biotechnol.*, 2022, **10**.
28. X. Tang, Y. Ravikumar, G. Zhang, J. Yun, M. Zhao and X. Qi, *Crit Rev Food Sci Nutr*, 2024, 1-28.